

# LIDAR TECHNIQUE AND MONITORING AT AIOFM, CHINA

Jun Zhou Shungxing Hu Dongsong Sun Huanling Hu

Anhui Institute of Optics and Fine mechanics, Chinese Academy of Sciences  
Hefei 230031, People's Republic of China jzhou@aiofm.ac.cn

## Abstract

This paper introduces a number of lidar systems, which are developed by Anhui Institute of Optics and Fine Mechanics, Chinese Academy of Sciences (AIOFM, CAS). It also presents jointed national projects and international cooperation programs on lidar monitoring for atmosphere at the AIOFM.

**Keywords:** Lidar, Atmospheric monitoring, Laser remote sensing

## 1. Introduction

Detection of the spatial and temporal distribution of greenhouse gases, aerosols, clouds is required for climate change and environmental assessment. Lidar can provide the vertical component of this distribution through advanced laser remote sensing.

In recent years, under supporting by Chinese Academy of Sciences, Ministry of Science and Technology of the People's Republic of China, and Ministry of Environmental Protection of the People's Republic of China, Anhui Institute of Optics and Fine Mechanics, Chinese Academy of Sciences (AIOFM, CAS) has developed many kinds of Lidar systems. These include Multiple-wavelength Mie scattering lidar, Polarization lidar, Micro Pulse Lidar, Raman lidar, Differential absorption lidar, Doppler lidar and Rayleigh-LIFluorescence lidar etc. By using these lidar systems, long-term, or field campaign, observations of aerosol, cloud, water vapor, O<sub>3</sub>, SO<sub>2</sub>, CO<sub>2</sub>, wind and temperature have been made.

AIOFM has also actively jointed in national and international cooperation projects on lidar monitoring for atmosphere. These are National Basic Research Program of China: Aerosol in China and its Climate Effect, Basic Scientific and Technical Data Sets: Measurements of Important Atmospheric Parameters with High Vertical Resolution in East China, SKYNET, AD-Net, CALIPSO validation program, and GALION.

This paper will introduce a number of these lidar systems and also present the lidar observed results in the above-mentioned projects.

## 2. Lidar systems

### 2.1 Two-wavelength lidar [1]

The lidar system is mainly composed of a two-wavelength Nd:YAG laser transmitter, a receiving optics, a signal receiver and a data-acquisition. Fig. 1 shows the schematic diagram of the lidar system.

AIOFM is one of the validation team members of the CALIPSO. The lidar system is used in the CALIPSO Quid Pro Quo (QPQ) validation program. Fig.2 presents Comparison of attenuated backscatter profiles at both 532nm (left figure) and 1064nm (right figure) wavelengths measured by this lidar and CALIPSO lidar nighttime at 02:11 Beijing time on Nov.24, 2007.

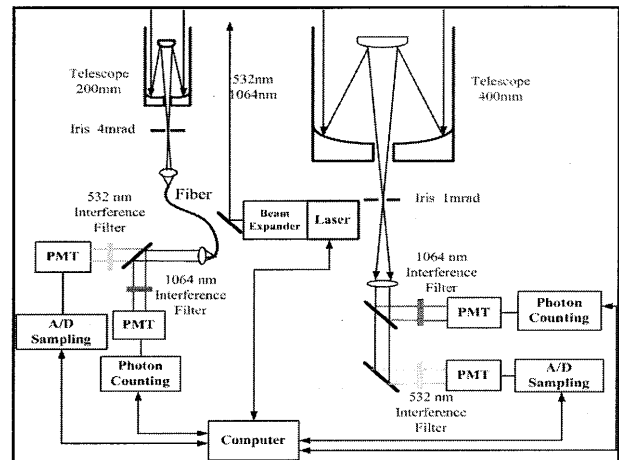


Fig.1. schematic diagram of the two-wavelength lidar.

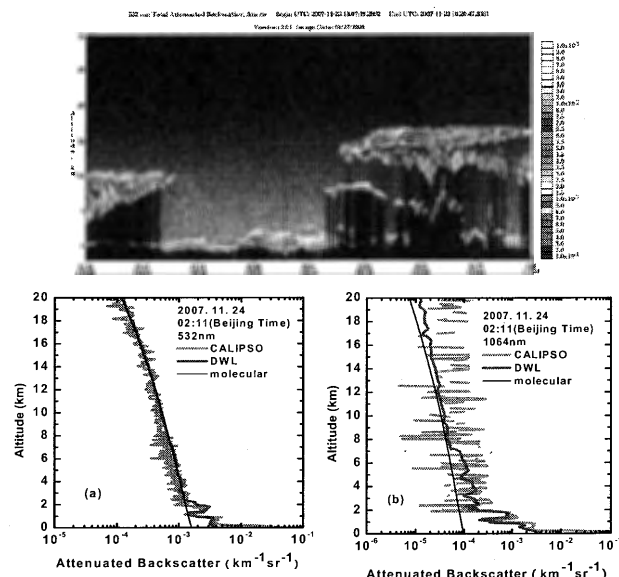


Fig. 2. Comparison of attenuated backscatter profiles during nighttime at 02:11 Beijing time on Nov. 24, 2007.

Fig.3 presents the Comparison results just for 532 nm wavelength during the daytime at 13:30 Beijing time on Nov.29, 2007 and at 13:32 Beijing time on March 20, 2008, respectively.

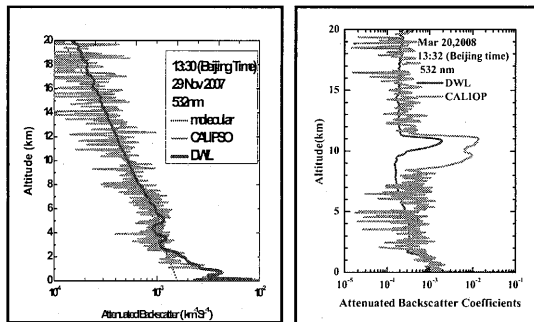
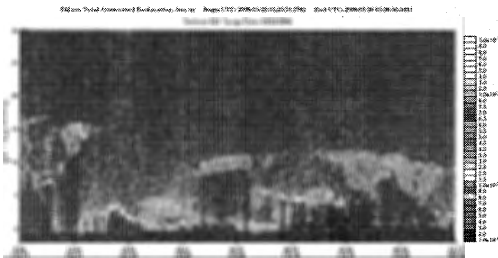


Fig.3. Daytime Comparison results at 532nm wavelength between CALIPSO and this lidar.

These Comparison results indicate that for both wavelengths the attenuated backscatter profiles measured by CALIPSO lidar generally agree well with the ones by our ground-based two-wavelength lidar during nighttime and daytime. The mixed layer was apparent by the CALIPSO lidar measurements.

However, the CALIPSO's attenuated backscatter profile at 1064 nm wavelength appeared large fluctuation in the upper troposphere because of lower signal- to -noise ratio.

### 2.2 Transportable Raman lidar [2]

The transportable Raman lidar system is used for measuring the vertical profiles of water vapor mixing ratio by Raman scattering. Fig. 4 shows the schematic diagram of the lidar system.

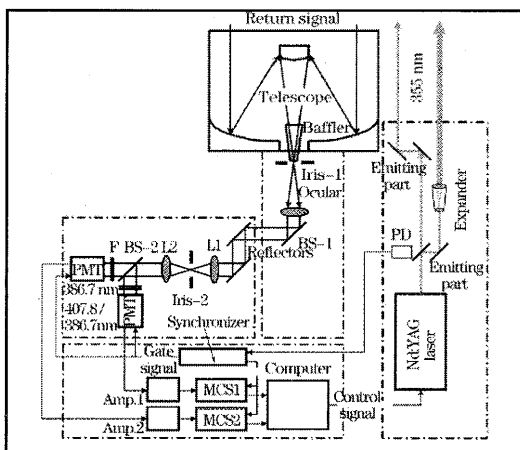


Fig.4. Schematic diagram of the Raman lidar system.

Fig. 5 (a) (b) presents the vertical profiles of water vapor mixing ratio measured by the Raman lidar at night on sep.12 (a) and Oct.9, 2004 in Hefei, respectively.

The radiosonde and another Raman lidar (L625) measuremental results are also shown in the figure for comparison.

The figure indicates that during the nighttime the Raman lidar can measure the water vapor mixing ratio from ground to about 8 km altitude.

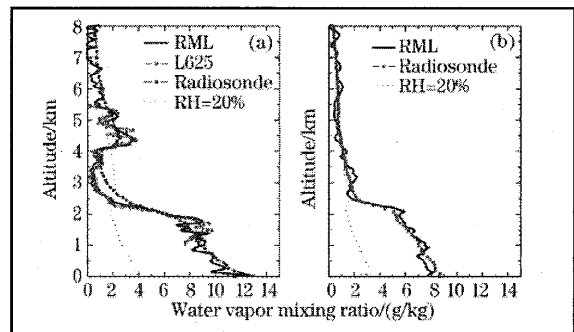


Fig. 5. Vertical profiles of water vapor mixing ratio at night on sep.12 (a), Oct.9 (b), 2004 in Hefei.

### 2.3 Mobile DIAL[3]

The Mobile DIAL is used for measurements of SO<sub>2</sub> and O<sub>3</sub> and NO<sub>2</sub> in the low troposphere. Fig. 6 shows photograph of the Mobile DIAL. Fig. 7 presents its schematic diagram.



Fig.6. Photograph of the Mobile DIAL.

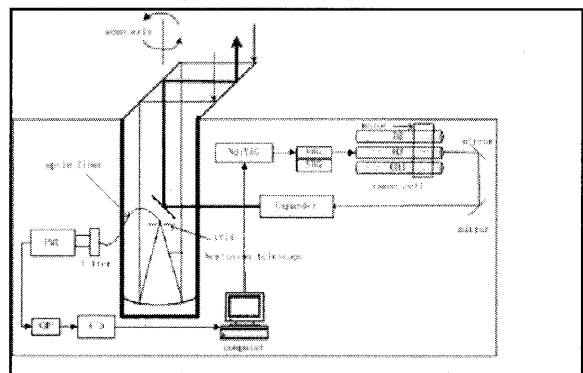


Fig. 7. Schematic diagram of the DIAL.

Fig. 8 presents the comparison results of vertical profiles of O<sub>3</sub> measured by this lidar with ozonesonde in Beijing on Nov. 5, 2004. Good agreement between them is apparent.

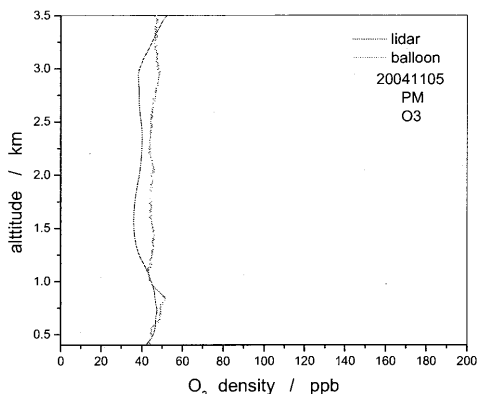


Fig. 8. Comparison results of vertical profiles of O<sub>3</sub> measured by the DIAL with ozonesonde in Beijing on Nov. 5, 2004.

#### 2.4 Doppler wind lidar[4]

The 1064nm aerosol Doppler wind lidar (DWL) system based on the double edge technique is capable of measuring three-dimensional wind profiles in the low troposphere. Fig. 9 presents its schematic diagram.

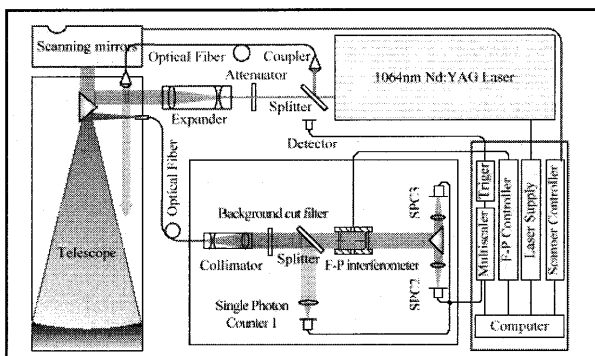


Fig. 9. Schematic diagram of the DWL.

A two axis mirror scanning system allows the lidar to achieve full sky coverage. Backscattered light is collected by a 30 cm diameter Cassegrain telescope. A dual Fabry-Perot etalon with a narrowband (0.5nm) interference filter is used to cut sky background radiation and provide a high spectral resolving element to measure the Doppler shift. A feedback circuit is developed and locks the laser frequency to the reference frequency.

The receiver for the frequency measurement is calibrated by the known line-of-sight Doppler shift produced from a rotating disk, and the calibration accuracy in velocity is less than 1% in the range of  $\pm 40\text{m/s}$ .

This system has line-of-sight wind speed dynamic

range of  $84\text{m/s}$  ( $\pm 42\text{m/s}$ ) and can measure wind profiles up to 10km altitude.

Comparison observations of the lidar wind profile were performed with CINRAD/SA Doppler weather radar, Airda16000 microwave radar and Vaisala balloon. Fig. 10 presents one of these observed results.

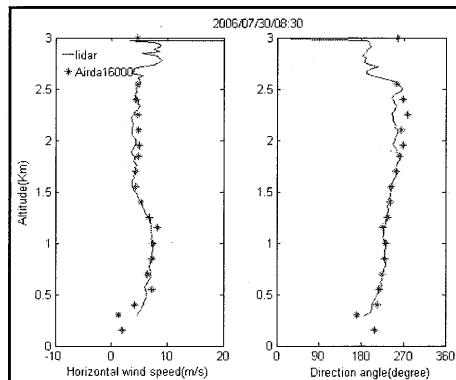


Fig.10. Profiles of wind speed and direction measured by DWL compared with data measured from Airda16000 Radar on July 30, 2006.

The Figure shows that in the altitude from 0.2km to 3 km, accuracies of wind vectors were better than 2m/s with 21.2m vertical resolution and 10 minute temporal resolution. Moreover, the accuracy, vertical resolution and temporal resolution can be improved with the current parameters of this lidar system.

Routine measurements have proved that DWL system is stable and reliable and has the capability of unattended automated measurements. Fig. 11 gives an example of continuing two-day observations by the lidar system.

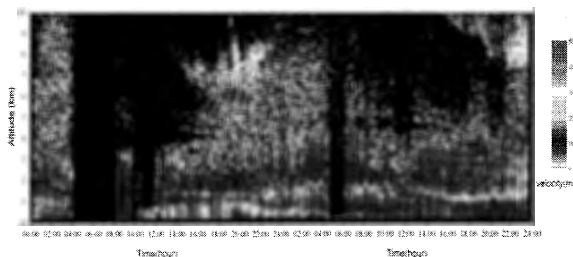


Fig.11 A color plot of two-day wind profiles measured by Doppler wind lidar from 00:00 of Apr.23 to 24:00 of Apr.24, 2006.

### 3. Lidar monitoring for atmosphere[5-10]

Anhui Institute of Optics and Fine Mechanics has actively joined in national and international projects on lidar monitoring for atmosphere.

These projects are:

National Basic Research program of China: Aerosol in China and its Climate Effect.

Basic Scientific and Technical Data Sets: Measurements of Important Atmospheric Parameters

with High Vertical Resolution in East China  
 SKYNET (SKY radiation observation NETWORK)  
 AD-Net (Asian Dust lidar observation NETWORK)  
 CALIPSO Quid Pro Quo (QPQ) validation  
 program, and  
 GALION (GAW Aerosol Lidar Observation  
 Network).

Here give an example. For the program of Aerosol  
 in China and its Climate Effect, seasonal average  
 aerosol backscatter coefficient profiles in Hefei have  
 been obtained from the lidar measurements. They are  
 shown in Fig. 12. It should be noted that the days with  
 cirrus clouds and Asian dusts have been removed from  
 the statistics. The figure clearly indicates that larger  
 aerosol backscatter coefficients were observed from 3  
 km to about 12km altitude range in the springtime rather  
 than any other season.

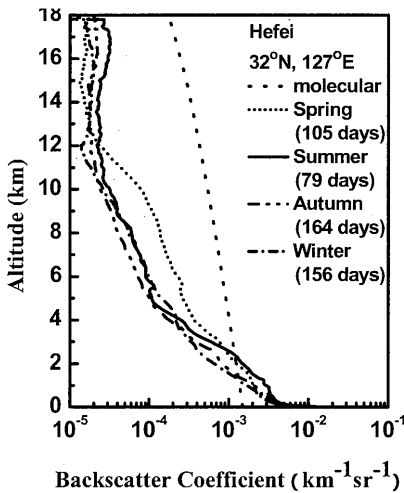


Fig.12. Seasonal average aerosol backscatter coefficient  
 profiles from 1998 to 2008.

The fitting to the above profiles for spring,  
 summer, autumn and winter can be expressed in the  
 following form:

$$\beta_o(z) = 3.92 \times 10^{-3} \exp\left(-\frac{z}{1.76}\right) + 1.00 \times 10^{-4} \exp\left[-\left(\frac{z-7.61}{3.39}\right)^2\right] + 1.60 \times 10^{-5} \exp\left[-\left(\frac{z-16.7}{4.78}\right)^2\right]$$

$$\beta_o(z) = 6.16 \times 10^{-3} \exp\left(-\frac{z}{1.32}\right) + 4.16 \times 10^{-5} \exp\left[-\left(\frac{z-8.56}{3.37}\right)^2\right] + 2.89 \times 10^{-5} \exp\left[-\left(\frac{z-16.5}{4.30}\right)^2\right]$$

$$\beta_o(z) = 4.36 \times 10^{-3} \exp\left(-\frac{z}{1.26}\right) + 3.36 \times 10^{-5} \exp\left[-\left(\frac{z-7.43}{4.99}\right)^2\right] + 1.96 \times 10^{-5} \exp\left[-\left(\frac{z-16.9}{3.99}\right)^2\right]$$

$$\beta_o(z) = 4.77 \times 10^{-3} \exp\left(-\frac{z}{1.04}\right) + 1.01 \times 10^{-4} \exp\left[-\left(\frac{z-4.18}{5.08}\right)^2\right] + 1.94 \times 10^{-5} \exp\left[-\left(\frac{z-15.6}{3.51}\right)^2\right]$$

Selected publications related to these projects are  
 presented in the References 5 through 10.

## REFERENCES

1. Bo Liu, Zhiqing Zhong and Jun Zhou, Development of a Mie scattering lidar system for measuring whole tropospheric aerosols, *Journal of Optics A: Pure and Applied Optics*, 9, 828-832, 2007.
2. Chenbo Xie, Jun Zhou, Guming Yue et. al., New Mobile Raman Lidar for Measurement of Tropospheric Water Vapor, *Acta Optica Sinica*, Vol.26, No.10. 2006 (in Chinese).
3. X. Liu, Y. Zhang, H. Hu, K. Tan, Z. Tao, S. Shao, K. Cao, G. Zhang Gaixia and S. Yu, Mobile lidar for measurements of SO<sub>2</sub> and O<sub>3</sub> in the low troposphere, *Optical Technologies for Atmospheric, Ocean, and Environmental Studies*, Daren Lu, Gennadii G. Matvienko; Eds. Proc. SPIE Vol. 5832, 156-163, May 2005.
4. D. Sun, Z. Zhong, J. Zhou, H. Hu, T. Kobayashi, Accuracy analysis of the Fabry-Perot etalon based Doppler wind lidar, *Optical Review*, Vol.12, No.5, 409-414, 2005.
5. J. Zhou, G. Yu, C. Jin, F. Qi, D. Liu, H. Hu, Z. Gong, G. Shi, T. Nakajima and T. Takamura, Lidar Observations of Asian Dust over Hefei, China in the Spring of 2000, *JGR*, 107, D15, AAC51-58, 2002.
6. J. Zhou, X. Qiu, G. Yu, C. Jin, F. Qi, Lidar Observations of Asian Dust over Eastern China (31.90° N, 117.160° E) from 1998 to 2001, *Lidar Remote Sensing In Atmosphere and Earth Sciences, reviewed and revised papers Presented at 21th ILRC, Quebec, Canada, 273-276*, 8-12 July, 2002.
7. D. Liu, F. Qi, C. Jin, G. Yue and J. Zhou, Polarization lidar observations of cirrus and Asian dust aerosols over Hefei, *Chinese Journal of Atmosphere Sciences*, Vol. 27, 1093-1100, 2003 (in Chinese).
8. S. Yuan, X. Yu, and J. Zhou, Lidar observations of the lower atmospheric layer in Hefei, *Chinese Journal of Atmosphere Sciences*, No.3, Vol. 29, 387-395, 2005(in Chinese).
9. J. Zhou, D. Liu, G. Yu, F. Qi, A. Fan, H. Hu, Z. Gong, G. Shi, T. Nakajima, T. Takamura, Seven years of Asian dust lidar observations over southeastern China, *Optical Technologies for Atmospheric, Ocean, and Environmental Studies*, Daren Lu, Gennadii G. Matvienko; Eds. Proc. SPIE Vol. 5832, 122-130, May 2005.
10. J. Zhou, D. Liu, G. Yue, F. Qi, A. Fan, H. Hu, Z. Gong, G. Shi: Vertical Distribution and Temporal Variation of Asian Dust Observed by Lidar over Hefei, China, *Journal of Korean Physical Society*, No.1, Vol. 49, 320-326, 2006.